Ionization of xenon Rydberg atoms at Au(111) surfaces: Effect of stray fields

D. D. Neufeld,[1] H. R. Dunham,[1] S. Wethekam,[2] J. C. Lancaster,[1] and F. B. Dunning[1]
[1]*Department of Physics and Astronomy, MS 61, Rice University, Houston, Texas 77005-1892, USA*
[2]*Institut für Physik, Humboldt-Universität zu Berlin, Newtonstr. 15, D-12489 Berlin, Germany*
(Received 10 January 2008; revised manuscript received 23 April 2008; published 22 September 2008)

The ionization of xenon Rydberg atoms excited to the lowest-lying state in the $n=17$ and 20 Stark manifolds at Au(111) surfaces is investigated as a function of the angle of incidence. Analysis of the data points to the presence of localized stray fields at the surface associated with surface inhomogeneities, which modify the atom-surface separation at which ionization occurs. A simple model is presented to justify this assertion and its implications are discussed.

DOI: 10.1103/PhysRevB.78.115423 PACS number(s): 79.20.Rf

I. INTRODUCTION

Charge exchange between atoms and surfaces plays an important role in many surface reactions and in many practical surface spectroscopies. Rydberg atoms in which one electron is excited to a state of large principal quantum number n provide a particularly sensitive probe of such charge exchange. At a conducting surface Rydberg atoms can be ionized by resonant tunneling of the excited electron into a vacant level in the surface. Because of their large physical size ($\sim n^2$ a.u.), such charge transfer can be quite rapid even relatively far from the surface. Also, the atomic energy levels are strongly perturbed by image-charge interactions, which influence the motion of the excited electron and distort the atomic wave functions.

Initial theoretical studies of Rydberg atom-surface interactions focused on hydrogen and showed that near a surface, hybridized "Stark-like" states are formed, the electron probability densities for some of which are strongly oriented toward the surface, others toward vacuum.[1–3] The tunneling rates, which depend critically on the overlap between the electronic wave function and the surface, were predicted to be many orders of magnitude greater for states oriented toward the surface. Experimental studies using xenon Rydberg atoms prepared in states oriented either toward or away from the surface, however, showed that the atoms ionize at similar atom-surface separations.[4] This was explained by calculations (for xenon) which showed that surface interactions lead to avoided crossings between neighboring levels with very different spatial characteristics as the surface is approached.[5–7] If as suggested by recent dynamical theory,[8] these crossings are traversed adiabatically, incident atoms successively assume the character of states oriented toward and away from the surface. They thus lose much of their initial identity leading all initial states to ionize at similar atom-surface separations. Subsequent measurements of absolute surface ionization efficiencies at near-grazing angles, α, to the surface ($\alpha \sim 4°$) showed that the data could be well fit by assuming that the charge transfer rate, on average, decreases exponentially as the atom-surface separation, Z, is increased.[9] Analysis of the data provided an estimate of the charge transfer rates and their dependence on atom-surface separation. While the resulting mean ionization distances were in good accord with theoretical predictions; the derived exponential decay lengths, Z_{decay}, for the charge transfer rate were somewhat larger than suggested by theory.[7,10] Recent measurements at Si(100) surfaces have shown that surface ionization signals can be influenced by the presence of stray "patch" fields[11,12] at the surface associated with surface charging or with contact potential differences due to surface inhomogeneities.[13,14] While the Au(111) surfaces employed earlier were atomically flat they were not atomically clean, raising the question as to whether stray fields might influence the results. To examine this question we have extended measurements at Au(111) surfaces to include a range of angles of incidence. The data point to the presence of localized stray electric fields at the surface. These modify the atom-surface separations at which ionization occurs and can account for the larger than expected exponential decay lengths reported earlier. A simple model is presented to justify this assertion

II. APPARATUS

The present apparatus is described in detail elsewhere.[9,15] Briefly, xenon Rydberg atoms are directed onto the Au(111) target surface at angles of incidence, α, relative to the surface, of $\sim 5-16°$. The Au(111) targets were obtained from a commercial vendor and were prepared by gold deposition on a cleaved mica substrate. They were mounted directly in the vacuum chamber following removal from their sealed packages. AFM measurements showed the target surfaces to be near atomically flat with a root-mean-square (rms) roughness of ≤ 0.3 nm over 1 μm. Ions formed at the surface are attracted to it by their image-charge fields. These fields are large and can rapidly accelerate an ion to the surface where it will be neutralized by an Auger process. To prevent this an ion collection field is applied perpendicular to the surface. Because the initial image-charge field experienced by an ion, and thus the external field required to counteract it, depends on the atom-surface separation Z at which ionization occurs, ionization distances can be inferred from measurements of the surface ionization signal as a function of the applied field.

The xenon Rydberg atoms are created by photoexciting the $^3P_0$ atoms contained in a tightly collimated mixed beam of Xe($^3P_{0,2}$) metastable atoms that is produced by electron impact excitation of ground-state xenon atoms contained in a supersonic expansion. The atoms are excited close to the

surface by the crossed output of an extracavity-doubled CR899–21 Ti:sapphire laser. Experiments are conducted in a pulsed mode by forming the output of the laser into a train of pulses of ~1 μs duration and ~3 kHz repetition rate using an A-O modulator. Excitation occurs in a weak dc field to allow creation of selected (oriented) Stark states. Here we excite the lowest member of the $n=17$ and 20 Stark manifolds, which correlate with zero-field f states and are initially strongly oriented toward the surface. Immediately after the laser pulse, a strong pulsed field of ~1 μs rise time and 20 μs duration is applied to establish the ion collection field. Since Rydberg atom flight times from their points of formation to the target surface are typically ~5–10 μs, arrival-time gating is used to discriminate against ions not formed in atom-surface interactions.

If ionization occurs at an atom-surface separation Z_i (and if no localized stray fields are present at the surface), the minimum external field that must be applied to overcome the image-charge attraction and prevent the ion striking the surface and being lost is (in a.u.)

$$E(Z_i,T_\perp)=\left\{\frac{1}{2Z_i}+\sqrt{\frac{T_\perp}{Z_i}}\right\}^2, \tag{1}$$

where $T_\perp \equiv mv_\perp^2/2$ is the kinetic energy of the atom perpendicular to the surface at the time of ionization. Thus by measuring the surface ionization signal as a function of ion collection field, the range of ionization distances can, in principle, be deduced. To obtain the absolute efficiency with which Rydberg atoms approaching the surface are detected as ions, the number of incident atoms is determined. This is accomplished by measuring the number of Rydberg atoms initially created by the laser using field ionization, which is induced by a large pulsed field applied immediately after the laser pulse. This number is then corrected for radiative decay during transit to the surface using the known (field-dependent) Rydberg atom lifetimes.[9]

III. RESULTS AND DISCUSSION

Figure 1 shows the applied-field dependence of the surface ion signals observed when xenon $n=17$ and $n=20$ Rydberg atoms are incident on a flat Au(111) target at the angles of incidence indicated. These signals are normalized to the number of Rydberg atoms that impact the surface. The sudden decrease in the surface ion signals seen at large applied fields is due to direct field ionization of the Rydberg atoms in vacuum before they reach the surface. The surface ion signals depend markedly on the angle of incidence. This is not unexpected because, as evident from Eq. (1), increases in the perpendicular component of ion kinetic energy lead to increases in the minimum external field required to prevent the ion from impacting the surface and being lost, i.e., to increases in the threshold ion collection field. However, for small angles of incidence each incident Rydberg atom can, with sufficiently large collection fields, be detected with near unit efficiency, indicating that each atom incident on the surface must undergo surface ionization.

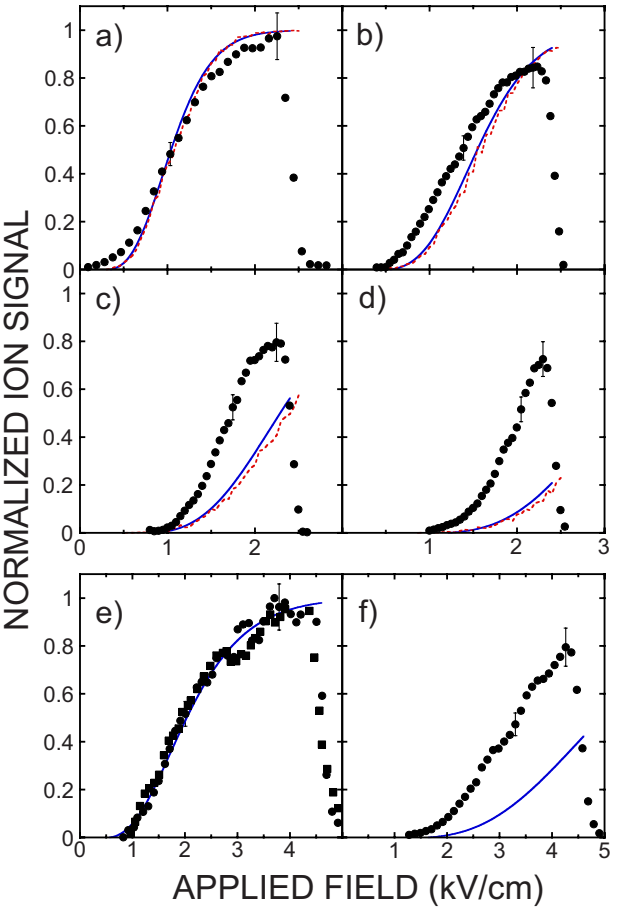

FIG. 1. (Color online) Applied-field dependence of the surface ion signals (●, ■) measured for Xe($n=20$) Rydberg atoms incident at near-grazing angles of incidence α of (a) 5°, (b) 8°, (c) 12°, and (d) 16° on an Au(111) surface. The lower panels show data for $n=17$ atoms incident at (e) 5° and (f) 14°. The measurements are normalized to the number of atoms that strike the target surface (see text). The solid and dashed lines show, respectively, results predicted using Eq. (2) and using the Monte Carlo model assuming the tunneling rates $\Gamma(Z,E)$ reported earlier (see text).

As shown previously,[9] the fraction of incident atoms that will be detected as ions using an ion collection field E can be written as

$$F(E)=1-\int_0^\infty f(v_\perp)\exp\left\{-\int_{Z_{\mathrm{crit}}(E,v_\perp)}^\infty \frac{\Gamma(Z',E)}{|v_\perp|}dZ'\right\}dv_\perp, \tag{2}$$

where $\Gamma(Z,E)$ is the ionization rate which depends both on the atom-surface separation Z and on the applied field, $f(v_\perp)$ is the known Rydberg atom velocity distribution, and Z_{crit} is related to E and $v_\perp$ by Eq. (1), i.e.,

$$Z_{\mathrm{crit}}=\frac{T_\perp}{4E}\left\{1+\sqrt{1+\frac{2\sqrt{E}}{T_\perp}}\right\}. \tag{3}$$

Given the sizeable number of avoided crossings between states with very different spatial characteristics that occur as the surface is approached, it is not unreasonable to approxi-

mate the ionization rate by some slowly varying overall average that, as suggested by hydrogenic theory, simply decreases exponentially with distance from the surface, leading to an expression for $\Gamma(Z,E)$ of the form

$$\Gamma(Z,E) = \Gamma_0(E)\exp\{-Z/Z_{\text{decay}}(E)\}. \quad (4)$$

In initial work $\Gamma_0(E)$ was taken to be a constant and $\Gamma(Z,E)$ written as

$$\Gamma(Z,E) = \Gamma_0 \exp\left\{-\frac{Z}{Z_{\text{decay}}(E)}\right\} = \Gamma_0 \exp\left\{-\frac{Z(1-kE_0)}{Z_{\text{decay}}(E=0)}\right\}, \quad (5)$$

where $E_0 \equiv n^4E$ is the ion collection field classically scaled to the principal quantum number of the incident atoms, and Γ_0 and $Z_{\text{decay}}(E=0)$ were taken as fitting parameters. The factor $(1-kE_0)$ included in $Z_{\text{decay}}(E)$ was designed to take into account the fact that, as will be discussed, the presence of the ion collection field lowers the potential barrier between the atom and surface, allowing a particular ionization rate to be achieved further from the surface. The value of $k=(4.2\times10^{-7}$ cm kV^{-1}) employed was derived from earlier calculations of the field dependence of the ionization rates for selected $n=10$ and $n=13$ hydrogenic states.[2,15] Fits to earlier data for $\alpha\sim4°$ yielded values of $Z_{\text{decay}}(E=0)$ of ~230 a.u. for $n=17$ and ~285 a.u. for $n=20$, both somewhat larger than suggested by theory. While, as evident from Fig. 1, use of these values yields reasonable fits to the present 5° data, they do not provide a good fit to the results at larger angles where the measured ion signals are significantly larger than those predicted, especially at the highest ion collection fields.

One possible reason for this discrepancy can be seen by using the simple classical over-the-barrier model,[16] which assumes that the ionization rate will jump from zero to infinity when the height of the potential barrier between the atom and surface dips below the electron energy. Consider the potential for the excited electron in a Rydberg atom located at a distance Z from the surface. For a line drawn perpendicular to the surface through the nucleus, this can be written

$$V(z) = -\frac{1}{|z|} - \left\{\frac{1}{4(Z+z)} - \frac{1}{4Z}\right\} + \left\{\frac{1}{2Z+z} - \frac{1}{2Z}\right\} + Ez, \quad (6)$$

where the origin of coordinates is taken to be the atomic nucleus. The various terms describe, respectively, the Coulomb interaction with the ion core, the interaction of the electron with its image charge, the interaction of the electron with the image charge of the core ion, and the effect of the ion collection field E. The form of this potential is shown in Fig. 2 for several values of applied field E and an atom-surface separation $Z=1250$ a.u. A potential barrier is evident between the atom and surface. For $E=0$, the top of the barrier lies at an energy of $\sim-1.39\times10^{-3}$ a.u., which is comparable to the binding energy of an $n=20$ Rydberg electron. This suggests that $n=20$ atoms will ionize at atom-surface separations $Z\sim1250$ a.u., consistent with earlier theoretical and experimental values. As the applied field is increased the height of the barrier is reduced allowing states of lower n to ionize at $Z=1250$ a.u. or, equivalently, states of a given n to ionize further from the surface.

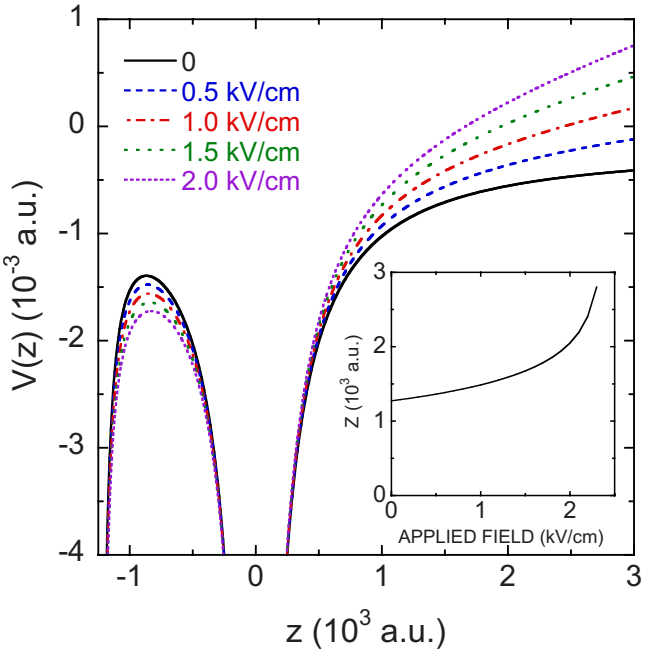

FIG. 2. (Color online) Position dependence of the electron potential, Eq. (6), for the values of applied ion collection field E indicated. The atom-surface separation Z is 1250 a.u. and the origin of coordinates ($z=0$) is taken to be the atomic nucleus. The inset shows the atom-surface separation Z at which the barrier height falls to -1.37×10^{-3} a.u. as a function of the applied field E.

The changes in barrier height induced by the presence of the ion collection field are illustrated in the inset in Fig. 2, which shows, as a function of applied field, the atom-surface separation Z at which the barrier height falls to -1.37×10^{-3} a.u.. This is equal to the effective binding energy of an $n=20$ atom inferred using the over-the-barrier model from the measured field ionization threshold in vacuum of ~2400 V cm^{-1}. The results in Fig. 2 therefore provide a measure of the atom-surface separation at which ionization of such atoms should occur, i.e., the ionization distance. At low applied fields a slow approximately linear increase is seen in the predicted ionization distances. These distances increase dramatically, however, as the applied field approaches the field ionization threshold. This latter effect is not taken into account in the expression for $\Gamma(Z,E)$ used earlier [Eq. (5)], which includes only a term linear in E. (This was not a serious omission in the earlier work because the ion collection efficiency was already ≥0.8 in the regime above ~1.5 kV cm^{-1} where the nonlinearity becomes important.)

In an attempt to include this effect, fits to the present data were undertaken using an expression for $\Gamma(Z,E)$ of the form

$$\Gamma(Z,E) = \Gamma_0 \exp\left\{-\frac{Z(1-kE_0-\ell E_0^2)}{Z_{\text{decay}}(E=0)}\right\} \quad (7)$$

that includes a term quadratic in E_0, where l is a constant derived from the fit. As illustrated in Fig. 3(a) for $n=20$, a

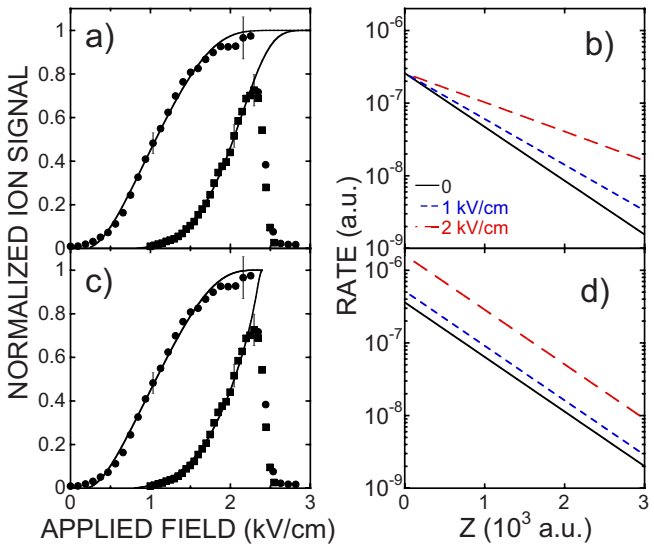

FIG. 3. (Color online) (a), (c) Fits to the experimental $n=20$ data for (●) $\alpha=5°$ and (■) $\alpha=16°$ obtained using the forms for $\Gamma(Z,E)$ shown in (a) Eq. (7) and in (c) Eq. (8). The corresponding ionization rates are presented in (b) and (d) for the values of E indicated (see text).

self-consistent fit to all the data can be obtained using an expression of this form. The corresponding ionization rates are shown in Fig. 3(b) for different values of applied field. Their decay lengths, however, are sizeable: $Z_{\text{decay}}(E=0)$ is ~590 a.u., $Z_{\text{decay}}(E=2\ \text{kV cm}^{-1})$ is ~1000 a.u. These are much larger than the values suggested by hydrogenic theory[2,10] (~30 a.u.) and are comparable to the atomic dimensions. Thus, while the data can be well fit using Eq. (7), the required decay lengths appear physically unreasonable.

An attempt was therefore made to fit the data assuming a fixed, field-independent decay length Z_{decay} and an expression of the form

$$\Gamma(Z,E) = \Gamma_0 \exp\left\{-\frac{Z - Z_{\text{OTB}}(E)}{Z_{\text{decay}}}\right\} = \Gamma_0(E)\exp\{-Z/Z_{\text{decay}}\} \tag{8}$$

with

$$\Gamma_0(E) = \Gamma_0 \exp\left\{\frac{Z_{\text{OTB}}(E)}{Z_{\text{decay}}}\right\}. \tag{9}$$

The "correction" term $Z_{\text{OTB}}(E)$ was obtained using the results in Fig. 2 and is the difference between the ionization distances predicted for an applied field E and for $E=0$. As illustrated in Fig. 3(c), good self-consistent fits to the data can be realized using an expression for $\Gamma(Z,E)$ of this form. The resulting ionization rates are shown in Fig. 3(d) but again point to decay lengths, $Z_{\text{decay}} \sim 550$ a.u., that are physically unreasonable.

IV. EFFECT OF STRAY FIELDS

The present observations can be accounted for by the presence of localized stray electric fields at the surface such as might arise from contact potential differences associated with surface inhomogeneities. Such fields modify the potential barrier between the atom and surface broadening the range of atom-surface separations at which ionization occurs. The scale lengths of the variations in surface potential important here must, however, be relatively large because ionization is expected to occur at atom-surface separations typically greater than ~60 nm (see Fig. 2). Electric fields associated with small-scale features on the surface such as steps,[17] while locally strong, decay rapidly with distance from the surface and are negligible at the distances of interest here.

Full evaluation of the effects of stray fields requires that the potential variations across the surface be known, which they are not. While it is likely that the scale lengths and amplitudes associated with these variations span a sizeable range, we demonstrate here that it is possible to account for the present observations using a simple periodic variation in potential across the surface. The surface is assumed to comprise an array of long parallel "wires" of equal width spaced by an amount equal to their width. The wires are embedded into the substrate such that the surface is flat and have potentials that alternate by $\pm\Delta V$ relative to that of the substrate. (Hardware and software limitations prevented loading fully three-dimensional potential and electric field arrays into the present calculations necessitating the consideration of a series of wires rather than some geometric arrangement of islands.) The equipotentials associated with this wire array were calculated using SIMION 3D 8.0. Representative results in a plane perpendicular to the surface and to the wires are shown in Fig. 4 for potential differences $\Delta V = \pm 80$ mV and wire widths of 0.5, 2.0, and 8.0 μm. The equipotentials show that for small feature sizes the magnitudes of the stray fields immediately above the wires can be sizeable. As the feature size increases the magnitudes of these near-surface fields decrease. However, the stray fields produced by large features decrease less rapidly with distance from the surface than for small features. In consequence, sufficiently far from the surface, the stray fields generated by large features, while small, become larger than those due to small features for the same feature potentials. For large feature sizes the stray fields are concentrated at the feature boundaries.

The presence of stray fields can have a dramatic effect on the height of the potential barrier between the atom and the surface which, based on the over-the-barrier picture, will lead to changes in the atom-surface separations at which ionization occurs. To estimate the effects of stray fields on ionization distances a simple two-dimensional model is adopted. This is not unreasonable as the incident atoms are in low-m states that are initially strongly oriented toward the surface. To determine ionization distances as a function of position across the surface, a series of perpendiculars to the surface were considered and were positioned along a line orthogonal to the wires. For each perpendicular the height of the potential barrier between atom and surface was determined as a function of atom position on the perpendicular. This was accomplished by evaluating the potential along a series of arcs of steadily increasing radius centered on the atom. For an atom a distance Z from the surface (and using the coordinate system shown in the inset whose origin is again taken

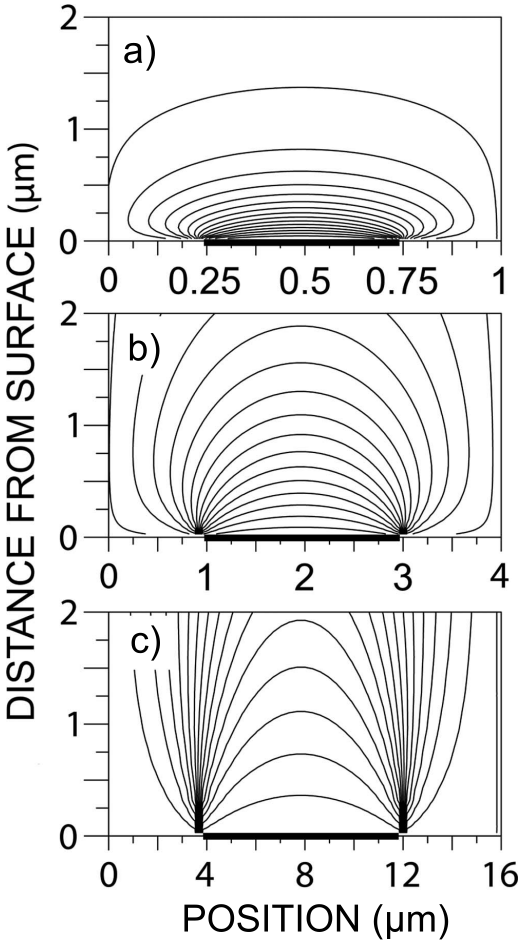

FIG. 4. Equipotentials above the positive wires in an array of parallel wires of (a) 0.5, (b) 2.0, and (c) 8.0 μm width spaced by amounts equal to their widths with alternating potentials of ± 80 mV relative to the substrate. These are drawn in a plane perpendicular to the surface and to the wires and are spaced by 5 mV. The bold lines indicate the extent of the features. Note that the scales of the horizontal and vertical axes are not the same.

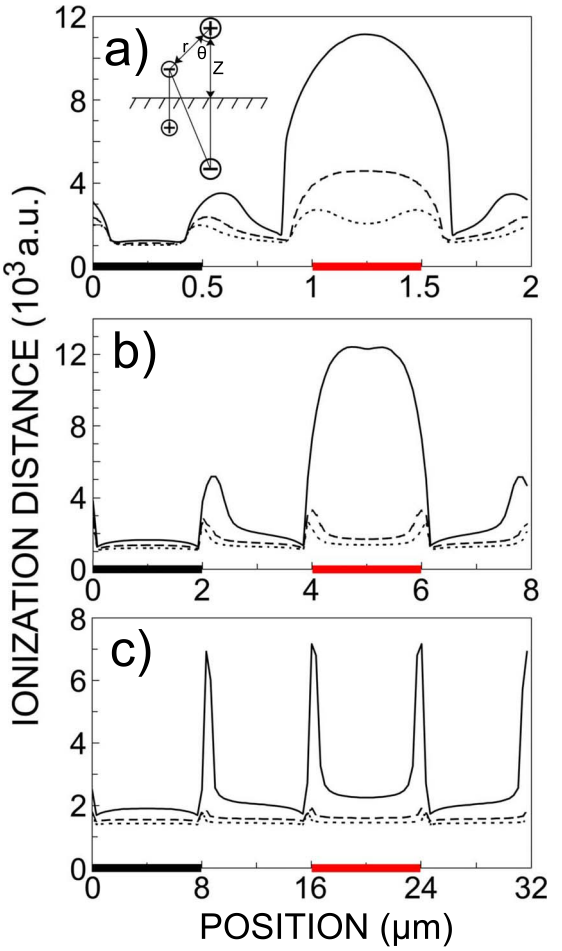

FIG. 5. (Color online) Ionization distances for $n=20$ atoms predicted by the classical over-the-barrier model for feature widths of (a) 0.5, (b) 2.0, and (c) 8.0 μm, potential differences ΔV of ± 80 mV, and ion collection fields of (- - - -) 0, (__ __ __) 1, and (_____) 2 kV cm^{-1} (see text). The bold lines indicate the feature positions (the negative feature is on the left). The inset shows the coordinate system used to compute the potential [Eq. (10)].

to be the atomic nucleus), the potential at any point on an arc of radius r is given by

$$V(r,\theta) = -\frac{1}{r} - \left\{\frac{1}{4(Z - r\cos\theta)} - \frac{1}{4Z}\right\} + \left\{\frac{1}{(4Z^2 + r^2 - 4Zr\cos\theta)^{1/2}} - \frac{1}{2Z}\right\} - Er\cos\theta - \{V_s(r,\theta) - V_s(0,0)\}, \quad (10)$$

where $V_s(r,\theta)$ is the potential associated with the surface potential discontinuities. Surface potentials were input to the calculation as a two-dimensional array from SIMION and interpolation employed to determine the potential at intermediate points. The potentials along arcs of increasing radius were calculated for values of θ in the range $\pm\pi/2$ and the minimum height of the potential barrier between atom and surface determined. (Since, as is evident from Fig. 4, the stray fields typically have a sizeable component parallel to the surface, this minimum does not generally lie on the perpendicular to the surface.) Ionization was deemed to occur at the atom-surface separation where for $n=17$ ($n=20$), the height of the potential barrier first fell below -1.83 (-1.37) $\times 10^{-3}$ a.u..

As illustrated in Fig. 5 for $n=20$ atoms, stray fields can lead, for the smaller feature sizes, to sizeable increases in the ionization distance above positive features. These become especially pronounced as the ion collection field approaches the threshold for field ionization. Above negative features the ionization distances are somewhat reduced. As expected, for large feature sizes the effects of stray fields on the ionization distance are most important at the feature boundaries. The present approach is different to that adopted in the earlier study[14] of oxidized Si(100) where a simple sinusoidal variation in ionization distance with position across the surface was assumed. Clearly, for large feature sizes such an approximation is not reasonable.

To explore the effects of stray-field-induced changes in ionization distance, a series of Monte Carlo simulations were undertaken, which followed the trajectories of the incoming

Rydberg atoms and of the product ions. The initial positions and velocities of the Rydberg atoms were selected at random from the known profiles of the laser and metastable atom beams and the known Rydberg atom velocity distribution. Each atom was propagated toward the surface (traveling in a plane perpendicular to the surface and orthogonal to the wires) taking into account the acceleration associated with the dipole-induced dipole interaction. (Tests revealed, however, that such accelerations are small at atom-surface separations greater than those typical of ionization and therefore make only small changes in the model predictions.) The trajectory of each incident atom was traced using a fourth-order Runge-Kutta (RK) algorithm until ionization occurred, which was assumed to happen where the trajectory of the incoming atom first intersected the ionization distance versus position curve (see Fig. 5) appropriate to the applied ion collection field. The position (and velocity) of the atom at ionization was then used as input to compute the subsequent trajectory of the product ion, which was again accomplished using a RK algorithm. The ion trajectory is governed by its image-charge field, the applied ion collection field, and local stray fields associated with surface inhomogeneities. To determine the latter the electric-field distribution associated with the surface features was input from SIMION as a two-dimensional array and the stray field at intermediate points determined by interpolation. In this manner the motion of the ion was followed until it either impacted the surface (and was presumed to be lost) or until it was sufficiently far from the surface that its collection by the applied field was guaranteed. Calculations for many initial atom trajectories were performed to determine the overall fraction of the incident Rydberg atoms that should be detected as ions for the particular angle of incidence, applied field, and stray-field conditions selected.

As an initial test of the Monte Carlo model, its predictions were compared directly (in the absence of any stray fields) to those obtained analytically using Eq. (2). To allow for the fact that ionization will occur over a range of atom-surface separations, the inverse cumulative distribution function method was employed. A random number between 0 and 1 was first selected. The probability of ionization during each successive element of the incoming path was determined using the tunneling rates $\Gamma(Z,E)$ obtained earlier. These probabilities were summed along the path and ionization deemed to occur when their sum first exceeded the preselected random number. The results of such model calculations are included in Fig. 1 and are in excellent agreement with those predicted analytically for the same conditions.

Surface ionization efficiencies were calculated using the full Monte Carlo model for a variety of feature sizes and potential differences. As illustrated in Fig. 6, those obtained using feature sizes of ~ 2 μm and potential differences of $\sim \pm 80$ mV provided good agreement with both the $n=17$ and the $n=20$ data. While the self-consistent fit evident in Fig. 6 is encouraging, especially given that $n=17$ and $n=20$ atoms ionize at rather different atom-surface separations requiring different ion collection fields, it serves only to show that the observed behavior can be accounted for by the presence of relatively small potential differences across the surface without the need to invoke large values of Z_{decay}. (In fact, for this simple over-the-barrier model Z_{decay} is effectively zero since it assumed that the ionization rate jumps from zero to infinity at a single distance.) In practice, incident atoms will encounter features with a range of sizes and potential differences. In the future more sophisticated models embodying a distribution of feature sizes and potential differences might be developed that would provide even better fits to the data. However, the present simple model clearly demonstrates that even small potential differences across a surface can play an important role in the ionization of Rydberg atoms. Indeed, given that the present Au(111) surfaces, while atomically flat, could not be cleaned in vacuum, it is perhaps remarkable that the effects of stray fields are not more pronounced.

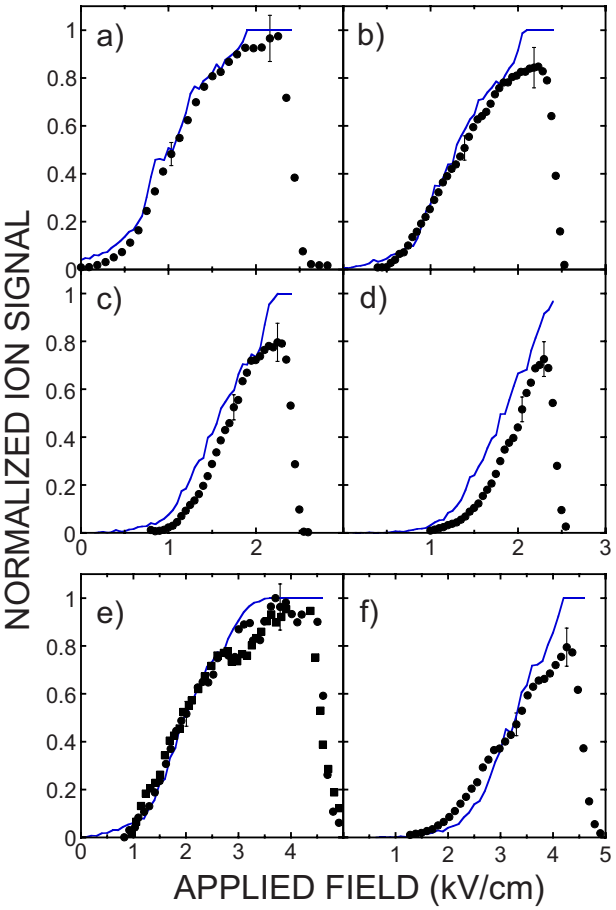

FIG. 6. (Color online) Comparison of surface ionization efficiencies calculated using the Monte Carlo model with experimental data (●, ■) for $n=20$ and angles of incidence, α, of (a) 5°, (b) 8°, (c) 12°, and (d) 16°, and for $n=17$ and angles of incidence of (e) 5° and (f) 14°. The model calculations were undertaken using feature widths of 2 μm and potential differences of $\Delta V = \pm 80$ mV (see text).

V. CONCLUSIONS

The present results illustrate the important role localized stray fields can play in surface ionization. Calculations for arrays of wires having widths of a few hundred nanometers to a few micrometers (which can be fabricated lithographi-

cally) and alternating potentials in the range of a few hundred millivolts to a volt using the present model suggest that localized surface fields might be exploited to efficiently detect low-n($n \leq 10$) atoms through surface ionization. Furthermore, the detection efficiency is predicted to depend markedly on whether the atoms are incident traveling parallel or perpendicular to the wires. Measurements at different azimuthal angles ϕ will therefore allow detailed testing of the present model and help evaluate the potential of Rydberg atoms for studying, for example, local electric fields produced by nanostructured surface arrays.

ACKNOWLEDGMENTS

Research was supported by the National Science Foundation under Grant No. PHY0650732 and by the Robert A. Welch Foundation under Grant No. C-0734.

[1] P. Nordlander, Phys. Rev. B **53**, 4125 (1996).
[2] P. Nordlander and F. B. Dunning, Phys. Rev. B **53**, 8083 (1996).
[3] P. Nordlander and F. B. Dunning, Nucl. Instrum. Methods Phys. Res. B **125**, 300 (1997).
[4] Z. Zhou, C. Oubré, S. B. Hill, P. Nordlander, and F. B. Dunning, Nucl. Instrum. Methods Phys. Res. B **193**, 403 (2002).
[5] C. Oubré, P. Nordlander, and F. B. Dunning, J. Phys. Chem. B **106**, 8338 (2002).
[6] F. B. Dunning, S. Wethekam, H. R. Dunham, and J. C. Lancaster, Nucl. Instrum. Methods Phys. Res. B **258**, 61 (2007).
[7] F. B. Dunning, H. R. Dunham, C. Oubré, and P. Nordlander, Nucl. Instrum. Methods Phys. Res. B **203**, 69 (2003).
[8] J. Sjakste, A. G. Borisov, and J. P. Gauyacq, Phys. Rev. A **73**, 042903 (2006).
[9] S. Wethekam, H. R. Dunham, J. C. Lancaster, and F. B. Dunning, Phys. Rev. A **73**, 032903 (2006).
[10] N. N. Nedeljkovic and Lj. D. Nedeljkovic, Phys. Rev. A **72**, 032901 (2005).
[11] J. B. Camp, T. W. Darling, and R. E. Brown, J. Appl. Phys. **69**, 7126 (1991).
[12] M. S. Rzchowski and J. R. Henderson, Phys. Rev. A **38**, 4622 (1988).
[13] H. R. Dunham, S. Wethekam, J. C. Lancaster, and F. B. Dunning, Nucl. Instrum. Methods Phys. Res. B **256**, 46 (2007).
[14] D. D. Neufeld, H. R. Dunham, S. Wethekam, J. C. Lancaster, and F. B. Dunning, Surf. Sci. **602**, 1306 (2008).
[15] S. B. Hill, C. B. Haich, Z. Zhou, P. Nordlander, and F. B. Dunning, Phys. Rev. Lett. **85**, 5444 (2000).
[16] J. Burgdörfer, P. Lerner, and F. W. Meyer, Phys. Rev. A **44**, 5674 (1991).
[17] B. Obreshkov and U. Thumm, Surf. Sci. **601**, 622 (2007).